

# Infrared and Raman spectroscopic imaging in biosciences

David Chenery and Hannah Bowring

Smith & Nephew Group Research Centre, York Science Park, Heslington, York YO10 5DF, UK

## Introduction

The function of biological tissue means it is inherently inhomogeneous. Even tissue normally thought of as uniform, like muscle, contains blood vessels and nerves while hard tissue, such as bone, can show varying degrees of mineralisation, which may be indicative of diseases such as osteoporosis. When one considers cells, the inhomogeneity is on a much smaller scale, with polysaccharide rich cell walls, cytoplasm containing a chemical soup rich in proteins and a tiny nucleus in which sugar phosphate heterocyclic containing polymers go about their business. Add to this the various chemicals that man may add to the system to heal, repair or kill undesirable cells or tissue, and the understanding of the concentration, distribution and effects of these additives becomes an analytical nightmare. Smith & Nephew is a company active in the healthcare industry, making devices principally for wound management, endoscopy and orthopaedics. Increasingly these devices are being used to facilitate active repair, and in order to understand and improve their efficacy we are employing a combination of infrared and Raman spectroscopic imaging.

An advantage of imaging is that the information is presented in a form readily comprehensible to non-spectroscopists and is comparable with the output of other microscopic techniques. The prime advantage in using the imaging function is that distribution of molecular species within a matrix can be determined quickly and at high lateral spatial resolution. Mapping, defined here as the sequential (in time) measurement of spectroscopic data point-by-point (even if data are presented as an image) is slow. Imaging as described here is performed in parallel and has a resulting multichannel advantage. The resulting image is recorded at a spatial resolution that is diffraction limited in an infrared measurement. Point-by-point mapping at this spatial resolution becomes extremely tedious.

Raman spectroscopy has two advantages over infrared for analysis of biological samples. Raman is less sensitive to water that is present in tissues and cells and sample preparation is easier. Scattering occurs from the surface region of the sample in Raman, whereas infrared requires microtomed sections (*c.* 10–20  $\mu\text{m}$  thick) for transmission or near-normal incidence reflection/absorption (“tranflectance”) measurements.

Just as in normal (non-imaging) spectroscopy, infrared and Raman spectroscopy are highly complementary. The two types of instrumentation differ in the modes of operation as well. The Raman instrument used at Smith & Nephew, a Renishaw System 2000 Microspectrometer, incorporates a Charge Coupled Device (CCD) as a detector. Once suitable analyte bands for the components of interest have been identified, the array nature of the CCD can be employed to determine their distribution by recording one image for each component sequentially.

Infrared imaging is performed using a multi-element detector. In our case, this is a Bio-Rad Stingray FT-IR instrument incorporating a  $128 \times 128$  ( $2^7 \times 2^7$ ) element Mercury Cadmium Telluride (MCT) focal plane array detector with a step-scanning interferometer. Thus 16,384 ( $2^{14}$ ) spatially-encoded interferograms are recorded simultaneously which are subsequently transformed to the same number of spectra. Though one might expect this to be time consuming, processing these at  $16 \text{ cm}^{-1}$  resolution occupies about 2.5 min for each sample. The principal difference for the user is that each pixel of the infrared data contains a complete spectrum ( $4000\text{--}1000 \text{ cm}^{-1}$ ), not just intensity data at a single wavelength as is the case with Raman.

In infrared imaging, the sampled size is  $750 \times 750 \mu\text{m}$ , giving a spatial resolution of approximately  $6 \mu\text{m}$ . This contrasts with the spatial resolution in Raman imaging which is the reciprocal of the wavelength of the laser used, in

our case HeNe at  $632.8 \text{ nm}$ , and is therefore  $0.6 \mu\text{m}$ .

As well as spatial resolution, sampling areas differ between the two techniques. The Raman microscope turret incorporates  $5\times$ ,  $20\times$  and  $50\times$  (transmitting) objectives, which can be employed to give sampled areas from  $40 \times 40 \mu\text{m}$  (at  $50\times$  magnification) to  $480 \times 480 \mu\text{m}$  (at  $5\times$  magnification). Spatial resolution in the infrared is effectively fixed by the requirement for large all-reflecting objectives. There is insufficient space to fit more than one of these on a microscope turret at any one time.

## Tissue adhesives

The use of cyanoacrylate tissue adhesives for skin closure is well known. There are concerns about the toxicity of the unreacted monomers and their rapid setting time can be disadvantageous if tissue has to be positioned accurately. We have investigated *ex vivo* the mechanism of cyanoacrylate adhesion to porcine cartilage utilising both infrared and Raman imaging. In order to retard the setting time of the adhesive, poly (methyl methacrylate) (PMMA) was added. This also increased the viscosity and it was anticipated that the tendency of the inherently low viscosity adhesive to penetrate too far into the tissue would be reduced. Raman images were recorded at shifts of  $2250 \text{ cm}^{-1}$  for cyanoacrylate and  $714 \text{ cm}^{-1}$  for PMMA. Figure 1(a) shows a Raman image of this formulation on tissue where the surface of the cartilage to which the adhesive was applied is at abscissa value of  $-30$ . This image shows that the cyanoacrylate still penetrated deeply into the cartilage, to approximately  $60 \mu\text{m}$ . Figure 1(b) shows that the PMMA has tended to concentrate in the outer  $20 \mu\text{m}$  (white and light yellow areas). This result provided a clear explanation of mechanical test data, in which the high viscosity formulation formed a weaker bond than the neat cyanoacrylate. The penetration depth of cyanoacrylate in cartilage in the Raman

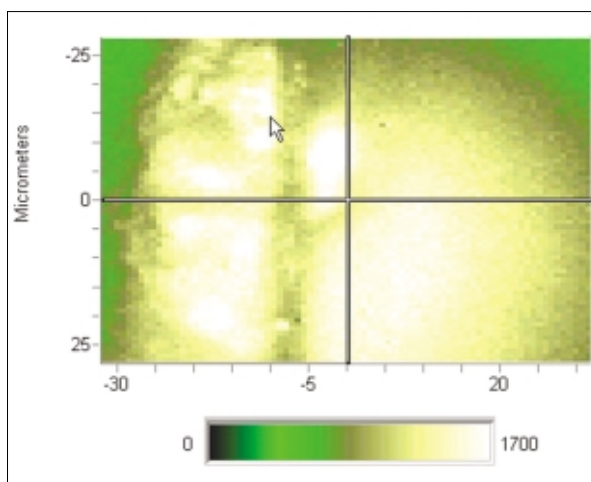


**Figure 1(a).** Raman image based on the distribution of the C-N band of viscosity modified cyanoacrylate applied to cartilage, (white highest concentration, yellow, grey and green progressively lower).

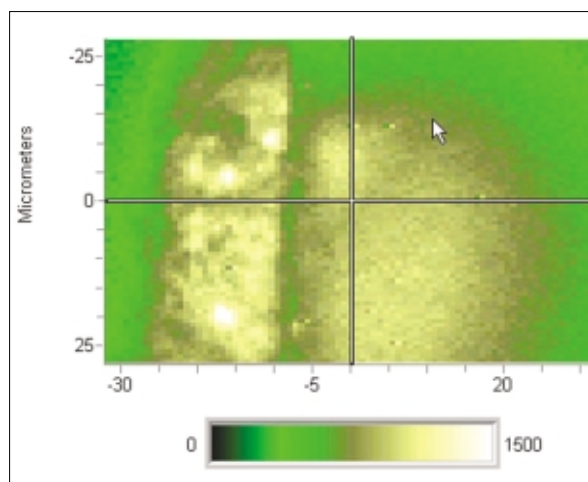


**Figure 1(b).** Raman image of the distribution of viscosity modifier (white highest concentration, yellow, grey and green progressively lower).

image correlated very well with the region of cell death observed using confocal light microscopy, which was also 60  $\mu\text{m}$ .

Alternatives to cyanoacrylates exhibiting slower setting and lower toxicity were tested. Siloxane chemistry offered some possibilities to meet these requirements. An infrared image of such an adhesive is shown in Figure 2 (the siloxane has no suitable Raman band). The strongest infrared absorption of the siloxane is a sharp band occurring at 1062  $\text{cm}^{-1}$  which overlaps with the broader glycan band occurring in cartilage. Even so, the infrared image plotted here at the frequency of the siloxane absorption relative to the polysaccharide showed a clear differentiation between the tissue (green area, upper) and the adhesive (red area, lower). The

boundary between the two is a sharp yellow line (indicating intermediate intensity). This result showed that there was very little penetration of the siloxane into the cartilage and thus a butt joint was formed. This result was confirmed by making individual measurements either side of the boundary. In Figure 2, the oval speckled objects in the upper part of the image are voids in the cartilage which are easily visible under the microscope. The process of ratioing the siloxane and polysaccharide bands produced this artefact.

Again, this result provided an explanation for the mechanical testing measurements in which the adhesive bond strength was approximately half of that of the cyanoacrylate. Thus, infrared and Raman imaging were combined to provide molecular explanations for bond-

ing strengths and cell toxicity of two tissue adhesives.

## Application to tissue analysis

### Hard tissue

Bone is a matrix of protein and a calcium phosphate mineral, hydroxyapatite, both of which are good infrared and Raman chromophores. Imaging can potentially be used to gain knowledge prior to attempting active repair as well as an indicator of success or otherwise of the treatment. Demineralisation of bone occurs in diseases like osteoporosis and knowledge of the distribution and amount of hydroxyapatite and protein is an indicator of the state of disease. Bone cements are commonly used in the repair of bone and joint replacement but tend to be exothermic when setting and may not represent the optimum solution. Spectroscopic imaging can assist in the design and evaluation of alternatives. The setting of cyanoacrylates is triggered by nucleophilic attack, most commonly by water but potentially by other nucleophiles such as  $-\text{NH}_2$  on the side chains of proteins. Water bonded to a cation is likely to be less nucleophilic than when associated with phosphate anions or protein. Knowing the distribution of protein and mineral in the surface of bone can determine whether or not a particular adhesive formulation will be effective and this type of information can be obtained from spectroscopic imaging.

In this particular example, Raman spectroscopy was the method of choice, due solely to the ease of sample present-

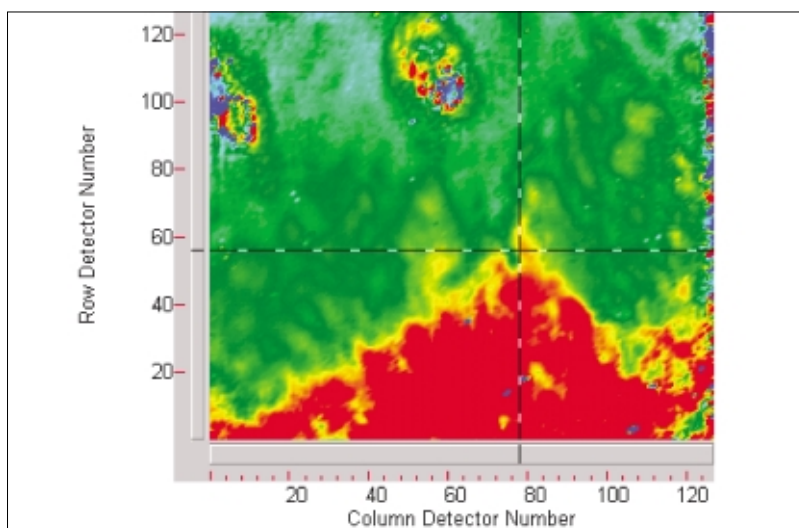


**Figure 2.** Infrared spectral image of siloxane adhesive applied to cartilage. Imaged area 720  $\times$  720  $\mu\text{m}$ .

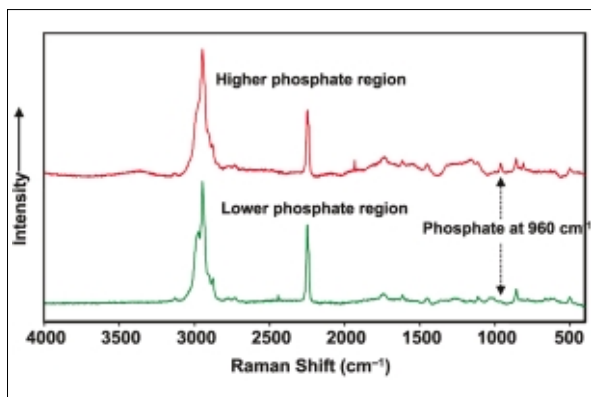


Figure 3. Raman spectra of two regions of bone treated with cyanoacrylate adhesive.

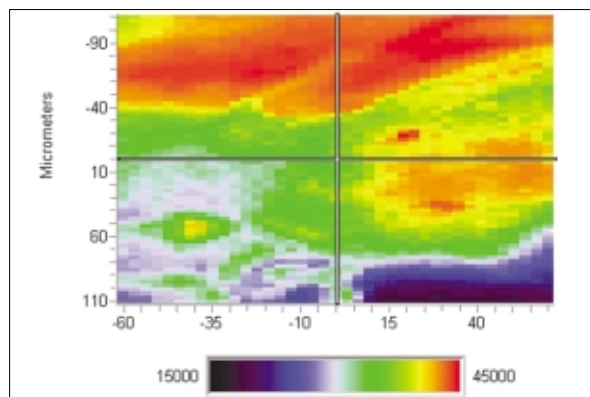


Figure 4. Distribution of phosphate in bone as determined by Raman spectroscopy (red highest, then orange, yellow and green to blue).

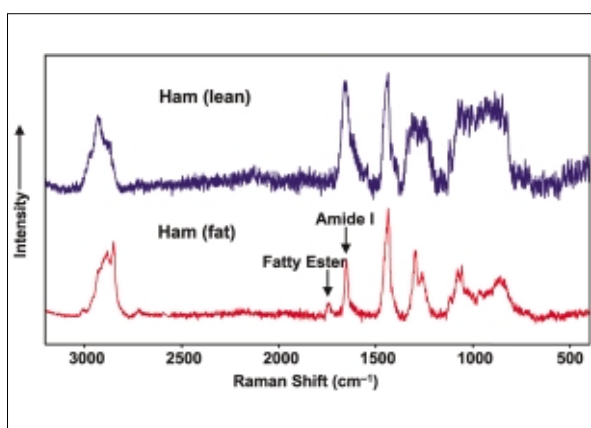


Figure 5. Raman spectra of fat and lean regions of ham.

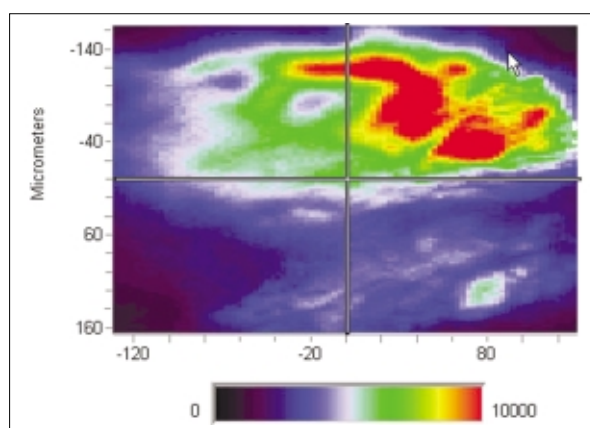


Figure 6. Raman image recorded at 1740 cm<sup>-1</sup> showing distribution of fat (green/yellow/red) in ham.

tation. Figure 3 shows Raman spectra of cyanoacrylate adhesive applied to trabecular bone. Inorganic phosphate exhibited a Raman band at 960 cm<sup>-1</sup> and it was noted that this varied considerably across the sample, as is shown in the accompanying image (Figure 4). It was noted that the cyanoacrylate band showed a slight difference in width depending whether it was on a phosphate-rich or phosphate-poor region.

These data show that images with high chemical specificity can be built up even where bands are fairly weak if one is prepared to scan for long enough.

### Soft tissue

Foodstuffs typically contain protein, fat and polysaccharide all of which have distinguishing bands in the infrared and Raman. Water is often a major constituent of biological tissues and this

may be a limiting factor in the case of infrared measurements, necessitating drying before analysis. Raman spectroscopy and imaging are very suitable alternatives. Figure 5 illustrates the Raman spectra of fat and lean regions of ham. The fat is shown by the presence of its ester band at 1740 cm<sup>-1</sup> and a sharp CH<sub>2</sub> band at 2847 cm<sup>-1</sup>. Examination of the spectra shows other distinguishing features in the 1200 and

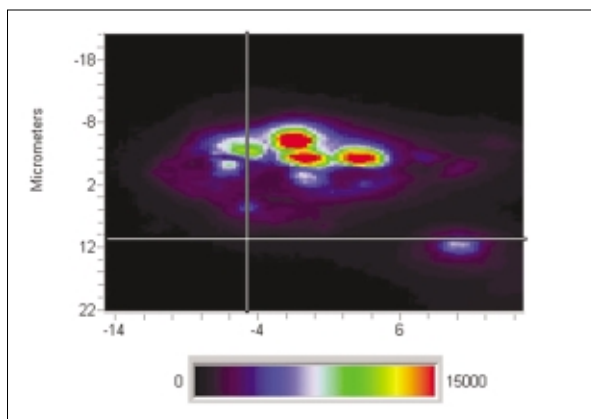


Figure 7. Yeast cells imaged at the frequency of the amide I band.

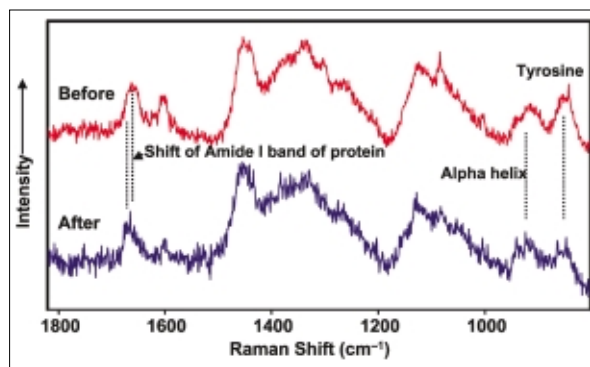


Figure 8. Raman spectra of yeast cells before and after treatment with ethanol.

1000  $\text{cm}^{-1}$  regions. The image in Figure 6 shows a very clear demarcation between the fat (red, yellow, green) and lean (blue) regions, the sample being placed so that the visual dividing line was at the ordinate of  $Y = 0$ . The spectra show that the protein band is weaker in the fat region, indicating partial replacement of protein by fat.

## Cells

As noted in the introduction, cells exhibit a range of biochemical species within a small volume, typically  $100 \mu\text{m}^3$ . Understanding cell biochemistry is a major area of investigation, with the disciplines of proteomics and metabolomics being very topical. Raman imaging is well placed to study cells, its high spatial resolution and relative freedom from interference by water being highly advantageous. Developments like confocal microscopy and Surface Enhanced Raman Scattering (SERS)<sup>1,2</sup> add to the advantages.

Elucidating the effects of physical or chemical stimuli as well as fundamental processes like mitosis or necrosis are amenable to study using Raman microspectroscopy in its basic form. Figure 7 displays a Raman image of yeast cells cultured on a metallic substrate imaged at the amide I (*c.*  $1650 \text{ cm}^{-1}$ ) frequency. The distribution of the cells is apparent. Changes in the cell were induced by treatment with absolute alcohol, killing them. Raman spectra of yeast before and after intoxication are shown in Figure 8. Chemical changes which can be detected are changes in the protein conformation from  $\alpha$ -helix to  $\beta$ -sheet<sup>1</sup> and the apparent loss of Tyrosine from the weakening of the 1600 and  $850 \text{ cm}^{-1}$  bands.

## Conclusions

Both infrared and Raman spectroscopy can be employed to investigate the biochemistry of inherently variable samples such as tissue and cells. An imaging capability adds a new dimen-

sion of being able to show visually the concentrations of components and of chemical treatments and to highlight their effects. The ability to produce the data in the form of a chemical image greatly aids the dissemination of information amongst colleagues acquainted with microscopic techniques but perhaps less familiar with spectroscopy. The key to producing these data is a thorough understanding of the spectra of the analytes, matrix and any interferences that may be present. Thus, spectroscopic expertise in the experimental phase is a must.

## References

1. G.J. Puppels, F.F.M. de Mul, C. Otto, J. Greve, M. Robert-Nicoud, D.J. Arndt-Jovin and T.M. Jovin, *Nature* **347**, 301 (1990).
2. T. Vo-Dinh, D.L. Stokes, G.D. Griffin, M. Volkan, U.J. Kim and M.I. Simon, *J. Raman Spectrosc.* **30**, 785 (1999).